

# Application of Kalman Filter Recurrent Neural Network for Identification and Control of Hydrocarbon Biodegradation Bioprocess

Ieroham Solomon Baruch<sup>1</sup>, Josefina Barrera Cortes<sup>2</sup>, and Carlos-Roman Mariaca Gaspar<sup>3</sup>

1. Department of Automatic Control, Center of Investigation and Advanced Studies, National Polytechnical Institute, Mexico

2. Department of Biotechnology and Bioengineering, Center of Investigation and Advanced Studies, National Polytechnical Institute, Mexico

3. ESIME-IPN, Mexico D.F., Mexico

**Abstract:** Biological treatment is attractive as a potentially low-cost technology, which converts toxic organic contaminants into CO<sub>2</sub> and biomass. Since the 70's, this technology has been applied for the hydrocarbon degradation, and today, it is considered as the best alternative to clean up polluted soils. For this bioprocess, one challenge is to provide enough O<sub>2</sub> and nutrients to enable rapid conversion of contaminants by either indigenous microorganisms or inoculated species. Another challenge is to achieve efficient contact between the active micro-organisms and the contaminants, which may represent a problem with in-situ treatment. An attractive alternative to overcome this problem is to apply a biological treatment in slurry phase using Horizontal Rotating Drum (HRD). Nowadays, semi empirical HRD models, based on the Monod equation, have been developed to predict micro-organism growth as a function of available contaminants concentration. However, as the application of such models requires experimental work for calculating the kinetics parameters involved, so an alternative modeling technique is required. The Kalman Filter Recurrent Neural Network Model (KF RNNM) offers many advantages as the possibility to approximate complex non linear high order multivariable processes, as the biodegradation process is. The KF RNNM has been applied for measurement data filtering and parameters plus state estimation of hydrocarbons biodegradation process, contained in polluted slurry, treated in a rotating bioreactor. Then the KF RNNM is simplified and used to design a Sliding Mode Control (SMC) of two-input two-output high order nonlinear plant. The KF RNNM learning algorithm is the dynamic Backpropagation one (BP). The graphical simulation results of the system approximation, and indirect adaptive neural control, exhibited a good convergence, and precise reference tracking.

**Key words:** hydrocarbon biodegradation bioprocess, horizontal rotating drum, identification and sliding mode control, Kalman filter recurrent neural network

## 1. Introduction

The Recent advances in understanding of the working principles of artificial neural networks has given a tremendous boost to identification, prediction and control tools of nonlinear systems [1-4]. The main network property namely the ability to approximate

complex non-linear relationships without prior knowledge of the model structure makes them a very attractive alternative to the classical modelling and control techniques. This property has been proved by the universal approximation theorem [5]. Among several possible network architectures the ones most widely used are the feed forward and the recurrent neural networks. In a feed-forward neural network the signals are transmitted only in one direction, starting from the input layer, subsequently through the hidden layers to the output layer, which requires applying a tap

---

**Corresponding author:** Ieroham Solomon Baruch, Ph.D., Associate Professor, research areas/interests: recurrent neural networks for identification and adaptive control of nonlinear plants. E-mail: baruch@ctrl.cinvestav.mx.

delayed global feedbacks and a tap delayed inputs to achieve a nonlinear autoregressive moving average neural dynamic plant model. A recurrent neural network has local feedback connections to some of the previous layers. Such a structure is suitable alternative to the first one when the task is to model dynamic systems, and the universal approximation theorem has been proved for the recurrent neural networks too. The preferences given to recurrent neural network identification with respect to the classical methods of process identification are clearly demonstrated in the solution of the “bias-variance dilemma” [5]. Furthermore, the derivation of an analytical plant model, the parameterization of that model and the Least Square solution for the unknown parameters have the following disadvantages: (a) the analytical model did not include all factors having influence to the process behavior; (b) the analytical model is derived taking into account some simplifying suppositions which not ever match; (c) the analytical model did not described all plant nonlinearities, time lags and time delays belonging to the process in hand; (d) the analytical model did not include all process and measurement noises which are sensor and actuator dependent. In Ref. [6] the method of invariant imbedding has been described. This method seemed to be a universal tool for simultaneous state and parameter estimation of nonlinear plants but it suffer for the same drawbacks because a complete nonlinear plant model description is needed.

So, the unknown nonlinear technological processes needed a new tool for modeling and identification capable to correlate experimental data and to estimate parameters and states in the same time, processing noisy measurements. Such efficient tool is the Kalman Filter Recurrent Neural Network (KF RNN), where the estimated parameters and states could be used directly for control [3, 7].

## 2. Recurrent Neural Network Methodology for Plant Modeling

### 2.1 Kalman Filter Recurrent Neural Network Topology and Learning

Block-diagrams of the Kalman Filter Recurrent Neural Network (KF RNN) model and its adjoined, are given in Fig. 1 and Fig. 2. Following Fig. 1 and Fig. 2, we could derive the dynamic Backpropagation (BP) algorithm of its learning using the diagramatic method [8].

Denoting by  $X$ ,  $Y$ ,  $U$  the state, output, and augmented input vectors with dimensions  $N$ ,  $L$ ,  $(M+1)$  and by  $Z$  the  $(L+1)$  — dimensional input of the feed-forward output layer, we can write the following equations for the KF RNN topology and learning:

$$X(k+1) = A_1X(k) + BU(k) - DY(k) \quad (1)$$

$$B = [B_1; B_0]; U^T = [U_1; U_2] \quad (2)$$

$$A_1 = \text{block-diag}(A_{1,i}), |A_{1,i}| < 1 \quad (3)$$

$$Z_1(k) = G[X(k)] \quad (4)$$

$$C = [C_1; C_0]; Z^T = [Z_1; Z_2] \quad (5)$$

$$V_1(k) = CZ(k) \quad (6)$$

$$V(k+1) = V_1(k) + A_2V(k) \quad (7)$$

$$A_2 = \text{block-diag}(A_{2,i}), |A_{2,i}| < 1 \quad (8)$$

$$Y(k) = F[V(k)] \quad (9)$$

$$W(k+1) = W(k) + \eta \Delta W(k) + \alpha \Delta W(k-1); |W_{ij}| < W_0 \quad (10)$$

$$E(k) = Y_d(k) - Y(k); E_1(k) = F'[Y(k)] E(k) \quad (11)$$

$$F'[Y(k)] = [1 - Y^2(k)] \quad (12)$$

$$\Delta C(k) = E_1(k) Z^T(k) \quad (13)$$

$$\Delta A_2(k) = E_1(k) V^T(k) \quad (14)$$

$$\text{Vec}(\Delta A_2(k)) = E_1(k) \circ V(k) \quad (15)$$

$$E_3(k) = G'[Z(k)] E_2(k); E_2(k) = C^T(k) E_1(k) \quad (16)$$

$$G'[Z(k)] = [1 - Z^2(k)] \quad (17)$$

$$\Delta B(k) = E_3(k) U^T(k) \quad (18)$$

$$\Delta D(k) = E_3(k) Y^T(k) \quad (19)$$

$$\Delta A_1(k) = E_3(k) X^T(k) \quad (20)$$

$$\text{Vec}(\Delta A_1(k)) = E_3(k) \circ X(k) \quad (21)$$

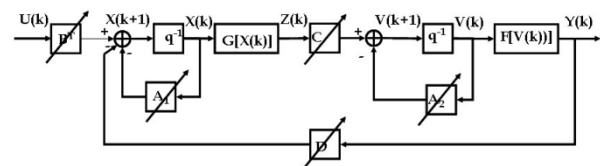


Fig. 1 Block-diagram of the KF RNN model.

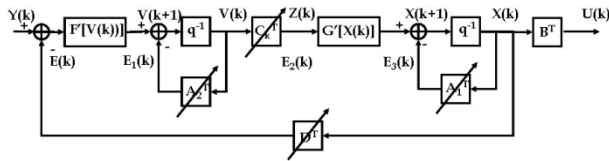


Fig. 2 Block-diagram of the adjointed KF RNN model.

where:  $Z_1$  and  $U_1$  are the  $(N \times 1)$  output and  $(M \times 1)$  input of the hidden layer; the constant scalar threshold entries are  $Z_2 = -1$ ,  $U_2 = -1$ , respectively;  $V$  is a  $(L \times 1)$  pre-synaptic activity of the output layer; the super-index  $T$  means vector transpose;  $A_1$ ,  $A_2$  are  $(N \times N)$  and  $(L \times L)$  block-diagonal weight matrices;  $B$  and  $C$  are  $[N \times (M+1)]$  and  $[L \times (N+1)]$  — augmented weight matrices;  $B_0$  and  $C_0$  are  $(N \times 1)$  and  $(L \times 1)$  threshold weights of the hidden and output layers;  $F[\cdot]$ ,  $G[\cdot]$  are vector-valued  $\tanh(\cdot)$  or sigmoid( $\cdot$ ) — activation functions with corresponding dimensions;  $F'[\cdot]$ ,  $G'[\cdot]$  are derivatives of the  $\tanh(\cdot)$  or sigmoid activation functions;  $W$  is a general weight, denoting each weight matrix ( $C$ ,  $A_1$ ,  $A_2$ ,  $B$ ,  $D$ ) in the KF RNN model, to be updated;  $\Delta W$  ( $\Delta C$ ,  $\Delta A_1$ ,  $\Delta A_2$ ,  $\Delta B$ ,  $\Delta D$ ), is the weight correction of  $W$ ;  $Y_d$  is an  $L$ -dimensional output of the approximated plant taken as a reference for KF RNN learning;  $\eta$ ,  $\alpha$  are learning rate parameters;  $\Delta C$ ,  $\Delta B$ ,  $\Delta D$ ,  $\Delta A_1$ ,  $\Delta A_2$  are weight corrections of  $C$ ,  $B$ ,  $D$ ,  $A_1$ ,  $A_2$ , respectively; the diagonals of the matrices  $A_1$ ,  $A_2$  are denoted by  $\text{Vec}(A_1(k))$ ,  $\text{Vec}(A_2(k))$ , respectively, where equations (15), (21) represented their learning as an element-by-element vector products;  $E$ ,  $E_1$ ,  $E_2$ ,  $E_3$ , are error vectors (see Fig. 2), predicted by the adjointed KF RNN model. The stability of the KF RNN model is assured by the activation functions  $[-1, 1]$  bounds and by the local stability weight bound conditions given by equations (3), (8). Here the input vector  $U$  and the input matrix  $B$  of the KF RNN are augmented so to fulfill the Kalman Filter requirements and the matrix  $D$  corresponded to the feedback gain matrix of the KF. The KF RNN is learnt applying the BP learning algorithm which is in fact an unrestricted optimization procedure, derived using the adjointed KF RNN (see Fig. 2) based on the Separation theorem [6], and the diagrammatic method [8].

### 2.2 KF RNN Methodology of Plant Identification and Sliding Mode Control

The block-diagram of the indirect adaptive neural control using the KF RTNN as plant identifier and a Sliding Mode Controller (SMC) is given in Fig. 3.

The stable nonlinear plant is identified by a KF RNN model with topology, given by equations (1)-(9) learned by the stable BP-learning algorithm, given by equations (10)-(21), where the identification error tends to zero. The simplification and linearization of the neural identifier equations (1)-(9), omitting the  $DY(\cdot)$  leads to the next local linear plant model, extracted from the complete KF RNN model:

$$X(k+1) = A_1 X(k) + BU(k) \quad (22)$$

$$Z(k) = H X(k); H = C G'(Z) \quad (23)$$

where  $G'(\cdot)$  is the derivative of the activation function and  $L = M$ , is supposed.

In Ref. [9], the sliding surface is defined with respect to the states variables and the SMC objective is to move the states from an arbitrary space position to the sliding surface in finite time. In Ref. [10], the sliding surface is also defined with respect to the states but the states of a SISO system are obtained from the plant outputs by differentiation. In Ref. [11], the sliding surface definition and the control objectives are the same. The equivalent control systems design is done with respect to the plant output, but the reach ability of the stable output control depended on the plant structure.

In Ref. [2], the sliding surface is derived directly with respect to the plant outputs which facilitated the equivalent SMC systems design.

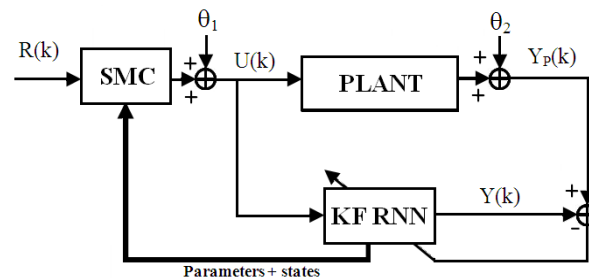


Fig. 3 Block — diagram of the control system containing KF RNN identifier and a sliding mode controller (SMC).

Let us define the following Sliding Surface (SS) as an output tracking error function:

$$S(k+1) = E(k+1) + \sum_{i=1}^P \gamma_i E(k-i+1), \quad |\gamma_i| < 1 \quad (24)$$

where:  $S(\cdot)$  is the Sliding Surface Error Function (SSEF) defined with respect to the plant output;  $E(\cdot)$  is the systems output tracking error;  $\gamma_i$  are parameters of the desired stable SSEF;  $P$  is the order of the SSEF. The tracking error and its iterate are defined as:

$$E(k) = R(k) - Z(k); \quad E(k+1) = R(k+1) - Z(k+1) \quad (25)$$

where  $R(k)$ ,  $Z(k)$  are  $L$ -dimensional reference and output vectors of the local linear plant model. The objective of the sliding mode control systems design is to find a control action which maintains the systems error on the sliding surface which assure that the output tracking error reaches zero in  $P$  steps, where  $P < N$ . So, the control objective is fulfilled if:

$$S(k+1) = 0 \quad (26)$$

Now, let us to iterate (23) and to substitute (22) in it so to obtain the input/output local plant model, which yields:

$$Z(k+1) = H X(k+1) = H [AX(k) + BU(k)] \quad (27)$$

From equations (24), (25), and (26) it is easy to obtain:

$$R(k+1) - Z(k+1) + \sum_{i=1}^P \gamma_i E(k-i+1) = 0 \quad (28)$$

The substitution of (27) in (28) gives:

$$R(k+1) - HAX(k) - HBU(k) + \sum_{i=1}^P \gamma_i E(k-i+1) = 0 \quad (29)$$

As the local approximation plant model (22), (23), is controllable, observable and stable, (see the preceding paragraph), the matrix  $A_1$  is diagonal, and  $L = M$ , then the matrix product  $(HB)$ , representing the plant model static gain, is nonsingular, and the plant states  $X(k)$  are smooth non-increasing functions. Now, from equation (29), it is easy to obtain the equivalent control capable to lead the system to the sliding surface which yields:

$$U_{eq}(k) = (HB)^{-1} [-HAX(k) + R(k+1) + \sum_{i=1}^P \gamma_i E(k-i+1)] \quad (30)$$

Following Ref. [9], the SMC avoiding chattering is taken using a saturation function instead of sign one. Here the saturation level  $U_0$  is chosen with respect to the load level perturbation. So the SMC takes the form:

$$U^*(k) = \begin{cases} U_{eq}(k), & \text{if } \|U_{eq}(k)\| < U_0 \\ -U_0 \frac{U_{eq}(k)}{\|U_{eq}(k)\|}, & \text{if } \|U_{eq}(k)\| \geq U_0 \quad i = 1 \end{cases} \quad (31)$$

It is easy to see that the substitution of the equivalent control (30) in the linear plant model (22), (23) showed an exact complete plant dynamics compensation which avoided oscillations, so that the chattering effect is not observed. Furthermore, the designed plant output sliding mode equivalent control substituted the multi-input multi-output coupled high order dynamics of the linearized plant with desired decoupled low order one.

### 3. Description of the Biodegradation Process in a Rotating Drum

Biological treatment is attractive as a potentially low-cost technology, which converts toxic organic contaminants into  $CO_2$  and biomass. Since the 70's, this technology has been applied for the hydrocarbon degradation, and today, it is considered as the best alternative to clean up polluted soils. For this bioprocess, one challenge is to provide enough  $O_2$  and nutrients to enable rapid conversion of contaminants by either indigenous microorganisms or inoculated species. Another challenge is to achieve efficient contact between the active micro-organisms and the contaminants, which may represented a problem with in-situ treatment. An attractive alternative to overcome this problem is to apply a biological treatment in slurry phase using Horizontal Rotating Drum (HRD) (Fig. 4).

The HRD can effectively mix heterogeneous blends of a wide range of particle sizes, and high solid concentration (more than 60%). The HRD operated with oxygen supply or aeration. Independently of the

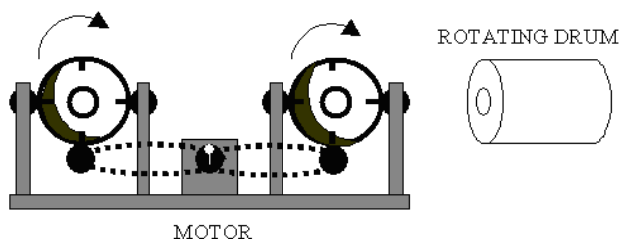


Fig. 4 Schematic diagram of a rotating drum system.

type of HRD operation (open or close), the insufficiency of water decreased the efficiency of hydrocarbon degradation in HRD favoring the formation of hydrocarbon balls [12, 13]. So one objective of the process control is to maintain the humidity at 60%, which is the maximal solid concentration determined as the best for hydrocarbon removal from polluted soils treated in open rotating slurry bioreactors [14]. Nowadays, semi empirical models, based on the Monod equation, have been developed to predict micro-organism growth as a function of available contaminants concentration. However, as the application of such models requires experimental work for calculating the kinetics parameters involved, so an alternative modelling technique is required. The RNNM offers many advantages as the possibility to approximate complex non linear high order multivariable processes, as the biodegradation process is. The bioremediation of polluted soils selected for modelling purpose was carried out by bio-stimulation in slurry phase using an open HRD. A silt loam (sand 36.5% w/w, silt 62.5% w/w and clay 1% w/w) soil of an average diameter of 15  $\mu\text{m}$ , particle diameter in the range 2-75  $\mu\text{m}$ , was used [14]. The soil was contaminated with 50000 ppm of crude oil collected from a contaminated zone located near from a petroleum refinery. The slurry was prepared with 40% weight of soil (715 g) and 60% weight of a mineral solution (formula in  $\text{kg}\cdot\text{m}^{-3}$ :  $(\text{NH}_4)_2\text{SO}_4$ , 19;  $\text{KH}_2\text{PO}_4$ , 1.7;  $\text{MgSO}_4$ , 1;  $\text{CaCl}_2\cdot 2\text{H}_2\text{O}$ , 0.005;  $\text{FeCl}_3\cdot 6\text{H}_2\text{O}$ , 0.0025; yeast extract, 0.59; tergitol -0.5%), (for more details, see Reg. [14]). The slurry was added to a HRD of 4 liters (13 cm diameter by 30 cm long), which was opened, on the flat faces, for a

natural air supply (see Fig. 4). The drum was operated during 19 days at a fix turning in the interval 3.5-20 RPM. During this time, the reactor was daily weight in order to replace the water lost, so to maintain constant the water concentration. Samples were removed each day for analysis of residual hydrocarbons, pH, water concentration and slurry viscosity. The hydrocarbon concentration was determined by an infrared spectrometer; the pH was measured with a Beckman  $\Phi$  potentiometer; water concentration was calculated by difference of two sequence data of the drum weight; finally, slurry viscosity was measured with an AND Vibro-viscometer SV-10 (MED BY A&D LTD). The biodegradation process was repeated at a different turning value (3.5, 5, 7.5, 10, 15, 20 RPM) in order to vary the oxygen available into the HRD.

## 4. Experimental and Simulation Results

### 4.1 Learning Pattern of KF RNN Training

The learning pattern (Fig. 5), used for RNNM training is composed by six input variables and three output variables. In order to avoid saturation problems in the RNNM training, the variables of the learning pattern are normalized in the interval 0-1.

The measured variables are: Residual Hydrocarbon Concentration (RH), Evaporated Water (EW); Soil Viscosity (VISC), Added Water (AW); Temperature (T); Velocity of Agitation (VA). The RNNM outputs are: OUT (RH, EW, VISC). Depending on the available measurements and the control objectives, this model could be simplified, where the input/output pattern is chosen as: ILP (RH, EW, AW, VA); OLP (RH, EW). This reduced model is used for sliding model control system design.

### 4.2 KF RNN HRD Identification and State Estimation Using Experimental Data

The described above learning algorithm is applied simultaneously to 4 fermentation kinetic data, represented by its input/output learning data patterns,



Fig. 5 Learning pattern for the KF RNN training.

and containing 19 points each (one per day). The total time of learning is 200 epochs, where the epoch size, corresponding to the number of data, is 76 iterations. After each epoch of training, the 4 sets are interchanged in an arbitrary manner from one epoch to another. The learning is stopped when the MSE% of learning and generalization reached values below 2%, and the relationship  $|\Delta W_{ij}(k)|/|W_{ij}(k)|*100\%$  reached values below or equal of 2% for all updated parameters. Graphical results of RNNM training are given in Fig. 6 for the last epoch of learning. In the graphics, the output variables of the RNNM are compared with the experimental data.

The Fig. 6a, b, c compared the 4 kinetics experimental data with those, issued by the RNNM. The output process data of 76 points are the hydrocarbon residual, the water requirements and the soil viscosity. The Fig. 6d represents the evolution of the mean squared error of approximation for whole learning process of 200 epochs. An unknown set of kinetic data, containing 19 points and repeated 4 times, so to maintain the same 76-points epoch size, is used as a validation (generalization) set, and these results are given on Fig. 7. The obtained graphical results of RNNM training and generalization shows a good convergence with an MSE% below 1.5% for learning and 2% for the generalization.

#### 4.3 Simulation Results of SMC Using the Identified Parameters and States

The simplified process model has been used to design a SMC system. The RNNM particular model has two inputs (AW, VA), two outputs (EW, RH) and nine states. The SSEF is chosen as a first order one ( $p = 1$ ) with parameters  $U_0 = 1, \gamma = 0.07, L = M = 2$ . The control variables (AW, VA) are given on Fig. 8 for 76

points. The graphical simulation results of the controlled system outputs (EW, RH), and the MSE%, also for 76 points, are given on Fig. 9.

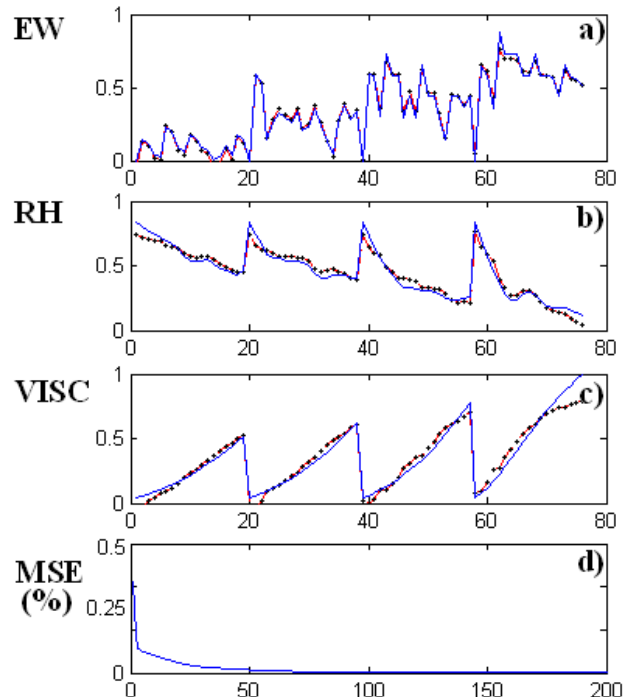


Fig. 6 Graphical results of KF RNN learning: a) EW; b) RH; c) VISC; d) MSE%.

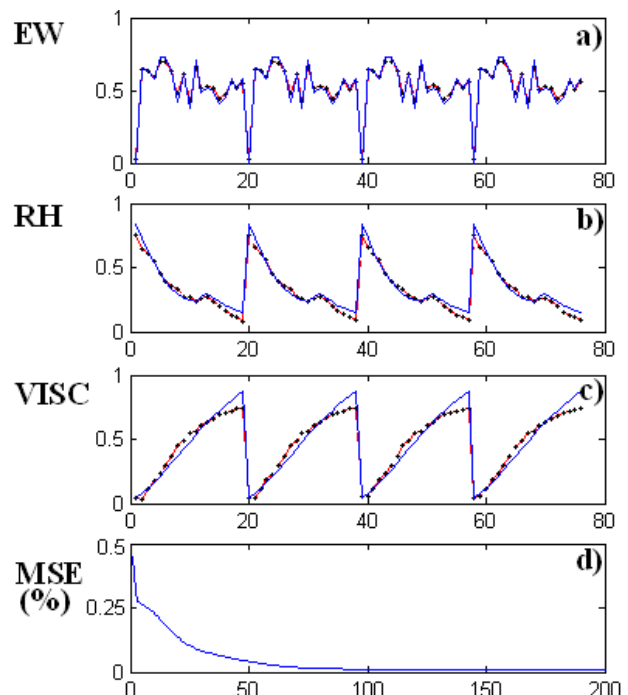


Fig. 7 Graphical results of KF RNN generalization. a) EW; b) RH; c) VISC; d) MSE%.

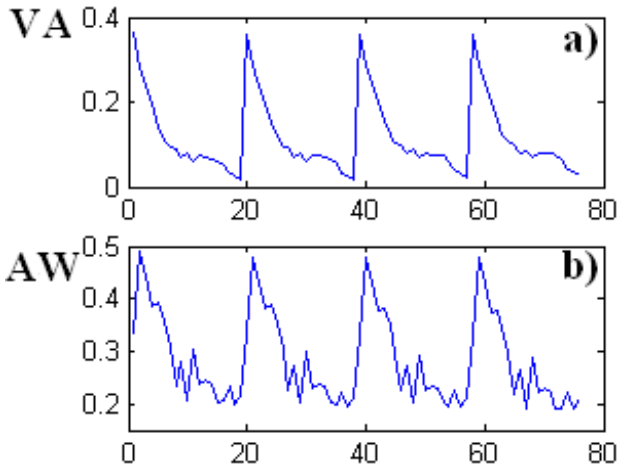


Fig. 8 Graphical results of SMC. a) VA; b) AW.

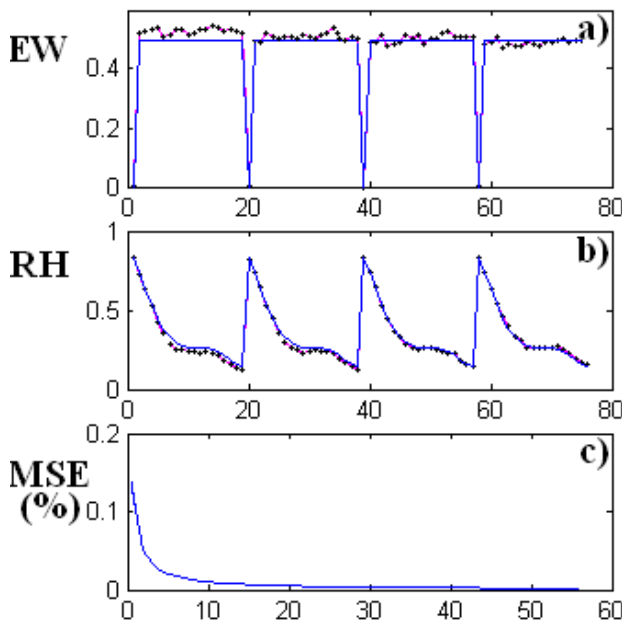


Fig. 9 Graphical results of SMC. a) EW; b) RH; c) MSE%.

The two system set points (continuous line) are compared with the plant outputs (EW, RH) (data point line) and are plotted subsequently for four sets of set-point data. The obtained MSE% of control at the end of the process is below 1%. The behavior of the control system in the presence of 5% white Gaussian noise added to the plant output has been studied accumulating some statistics of the final MSE% ( $\xi_{av}$ ) for multiple run of the control program, which results are given on Table 1 for 20 runs.

Table 1 Final means squared error (%) of control ( $\xi_{av}$ ) for 20 runs of the control program.

No	1	2	3	4	5
MSE%	0.6434	0.6577	0.7669	0.6805	0.6662
No	6	7	8	9	10
MSE%	0.5757	0.5835	0.7043	0.7040	0.6350
No	11	12	13	14	15
MSE%	0.6602	0.7759	0.7732	0.6566	0.6408
No	16	17	18	19	20
MSE%	0.6481	0.6061	0.7240	0.6514	0.5725

The mean average cost for all runs ( $\epsilon$ ) of control, the standard deviation ( $\sigma$ ) with respect to the mean value and the deviation ( $\Delta$ ) are given by the following formulas:

$$\epsilon = \frac{1}{n} \sum_{k=1}^n \xi_{avk} \quad \sigma = \sqrt{\frac{1}{n} \sum_{i=1}^n \Delta_i^2} \quad (32)$$

$$\Delta = \xi_{av} - \epsilon; \quad \epsilon = 0.6663 \%; \quad \sigma = 0.0593\% \quad (33)$$

where: k is the run number and n is equal to 20.

## 5. Conclusion

This paper proposes a new full order observer-filter RNNM with closed loop topology for state and parameter estimation and measurement noise filtering of hydrocarbon degradation process carried out in a rotating drum system. The proposed KF RNNM has six inputs, three outputs and nine neurons in the hidden layer, with global and local feedbacks. The BP learning algorithm is derived using the diagrammatic method and the adjoined RNNM. Then the obtained RNNM is simplified and used to design a SMC. The RNNM particular model has two inputs (AW, VA), two outputs (EW, RH) and nine states. The SSEF is chosen as a first order one ( $p = 1$ ) with parameters  $U_0 = 1, \gamma = 0.07, L = M = 2$ . The experimental and simulation identification and control results obtained exhibited a good convergence and precise reference tracking. The MSE% of the KF RNNM learning and generalization is below 1.5% (2% for generalization) and the MSE% of control is below 1%. The behavior of the control system in the presence of 5% white Gaussian noise added to the plant output has been studied accumulating some statistics of

the final MSE% ( $\xi_{av}$ ) for multiple run of the control program, which results are given on Table 1 for 20 runs. The mean average cost for all runs ( $\epsilon$ ) of control, the standard deviation ( $\sigma$ ) with respect to the mean value and the deviation ( $\Delta$ ) are obtained as  $\Delta = \xi_{av} - \epsilon$ ;  $\epsilon = 0.6663\%$ ;  $\sigma = 0.0593\%$ . The results could be improved augmenting the number of measurement points per fermentation and augmenting the number of fermentations per epoch.

## References

- [1] I. S. Baruch, P. Genina-Soto and J. Barrera-Cortes, Predictive neural model of an osmotic dehydration process, *Journal of Intelligent Systems* 14 (2-3) (2005) 143-155.
- [2] I. S. Baruch, A. Hernandez, C. R. Mariaca-Gaspar and B. Nenkova, An adaptive sliding mode control with I-term using recurrent neural identifier, *Cybernetics and Information Technologies, BAS* 7 (1) (2007) 21-32.
- [3] J. D. Boskovic and K. S. Narendra, Comparison of linear, nonlinear and neural-network-based adaptive controllers for a class of fed-batch fermentation processes, *Automatica* 31 (1995) 817-840.
- [4] R. De la Torre-Sanchez, I. S. Baruch, J. Barrera-Cortes, Neural prediction of hydrocarbon degradation profiles developed in a biopile, *Expert Systems with Applications* 31 (2006) 283-389.
- [5] S. Haykin, *Neural Networks: A comprehensive Foundation* (2nd ed.), Prentice-Hall, Upper Saddle River, New Jersey 07458, 1999. pp. 84-89, 208-213.
- [6] A. P. Sage, *Optimum Systems Control*, Prentice-Hall Inc., Englewood Cliffs, New Jersey, 1968.
- [7] K. S. Narendra and K. Parthasarathy, Identification and control of dynamic systems using neural networks, *IEEE Transactions on Neural Networks* 1 (1) (1990) 4-27.
- [8] E. Wan and F. Beaufays, Diagrammatic method for deriving and relating temporal neural networks algorithms, *Neural Computations* 8 (1996) 182-201.
- [9] C. Eduards, S. K. Spurgeon and R. G. Hebden, On the design of sliding mode output feedback controllers, *International Journal of Control* 76 (9/10) (2003) 893-905.
- [10] A. Levent, Higher order sliding modes, differentiation and output feedback control, *International Journal of Control* 76 (9/10) (2003) 924-941.
- [11] K. D. Young, V. I. Utkin and U. Ozguner, A control engineer's guide to sliding mode control, *IEEE Trans. on Control Systems Technology* 7 (3) (1999) 328-342.
- [12] M. Alexander, *Biodegradation and Bioremediation*, Academic Press, New York, 1999.
- [13] J. T. Cookson, *Bioremediation Engineering: Design and Application*, Mc Graw-Hill, New York, 1995.
- [14] E. Manilla-Pérez, H. M. Poggi-Varaldo, B. Chávez-Gómez, F. Esparza-García and J. Barrera-Cortés, Evaluation of a rotatory drum, used for bioremediation of a hydrocarbon contaminated soil (in Spanish), *Interciencia* 29 (9) (2004) 515-520.